

Conditions for State and Control Constraint Activation in Coordination of Connected and Automated Vehicles

A M Ishtiaque Mahbub, *Student Member, IEEE*, Andreas A. Malikopoulos, *Senior Member, IEEE*

Abstract—Connected and automated vehicles (CAVs) provide the most intriguing opportunity to reduce pollution, energy consumption, and travel delays. In earlier work, we addressed the optimal coordination of CAVs using Hamiltonian. In this paper, we investigate the nature of the unconstrained problem and provide conditions under which the state and control constraints become active. We derive a closed-form analytical solution of the constrained optimization problem and evaluate the solution using numerical simulation.

I. INTRODUCTION

The implementation of an emerging transportation system with connected automated vehicles (CAVs) enables a novel computational framework to provide real-time control actions that optimizes energy consumption and associated benefits. From a control point of view, CAVs can alleviate congestion at major transportation segments [1], reduce emission, improve fuel efficiency [2], [3], and increase passenger safety. Partially constrained optimal control of CAVs reduces computational complexity, but may degrade the performance metrics in real-world application. Particularly, vehicle speed and acceleration/deceleration constraints directly affect the physical limitations of the system, traffic regulations and passenger comfort. Therefore, we need to address the problem of optimal control of CAVs with hard constraint on vehicle state and control.

Intersections, merging roadways, roundabouts, and speed reduction zones along with the driver responses to various disturbances [4] are the primary sources of bottlenecks that contribute to traffic congestion. Several research efforts have been reported in the literature proposing either centralized or decentralized approaches on coordinating CAVs through the conflict scenarios to improve traffic condition. In 2004, Dresner and Stone [5] proposed the use of the reservation scheme to control a signal-free intersection of two roads. Since then, several research efforts have extended this approach [6]–[8]. Some approaches have focused on coordinating vehicles at intersections to improve the traffic flow [9]–[11]. Detailed discussions of the research reported in the literature to date on coordination of CAVs to improve vehicle-level operation can be found in [12].

More recently, an optimal control framework was established for coordinating online CAVs in different transportation segments. A closed-form, analytical solution without

considering state and control constraints was presented in [13], [14] for coordinating online CAVs at highway on-ramps, in [15], [16] at intersections, and in [17] at roundabouts. The solution to the state and control unconstrained optimization problem discussed above shows acceleration spikes (jerk) at the boundaries of the solution, possibly exceeding the vehicle’s physical limitation and giving rise to undesired passenger discomfort. Additionally, the unconstrained optimal solution only abides by the roadway speed limit at the predefined terminal points and fails to maintain the roadway regulation within the control zone.

Therefore, the unconstrained optimal solution may not be admissible in real-world application. To mitigate terminal jerk, Ntousakis, Nikolos, and Papageorgiou [14] reformulated the optimal control problem with vehicle acceleration as an additional state and using jerk as the control input. This approach provides safe state/control values at the terminal points, but can not guarantee that the state and control constraints will not become active within the optimization horizon. The optimal control problem considering state and control constraints was addressed in [3] at an urban intersection. However, the resulting formulation relies on stitching the unconstrained and constrained arcs together, and suggests recursive computation of the analytical solution until all of the constraint activations are resolved. This procedure can lead to a complex structure of the analytical solution at every recursion. Moreover, this recursive procedure of recalculating the controller constants can become computationally exhaustive, preventing possible real-time implementation of the particular framework.

Therefore, in this paper, we investigate the formulation presented in [3] to provide useful insights about the state and control constraint activation to increase computational efficiency, and derive closed form analytical solution using the Hamiltonian analysis. In particular, we (1) provide conditions under which the constraint activation space can be reduced, (2) provide conditions under which specific combination of state and control constraint activation can be identified to avoid redundant calculation, and (3) derive a closed form analytical solution for the constrained optimization problem under different cases of constraint activation identified in (2). Finally, we validate the effectiveness of the analysis and the corresponding optimal solution in simulation environment.

The remainder of the paper is organized as follows. In Section II, we introduce the general optimization problem formulation and present the unconstrained case. In Section III, we discuss different aspects of the state and control constrained formulation in detail. In Section IV, we provide

This research was supported by ARPAC’s NEXTCAR program under the award number DE-AR0000796.

The authors are with the Department of Mechanical Engineering, University of Delaware, Newark, DE 19716 USA (emails: mahbub@udel.edu; andreas@udel.edu.)

the analytical solution of the constrained optimization. In Section V, we evaluate the effectiveness of the proposed approach in a simulation environment. We draw conclusions and discuss next steps in Section VI.

II. PROBLEM FORMULATION

We consider a network of CAVs cruising through a roadway containing a four-way intersection, as shown in Fig. 1. Although we adopt a specific scenario for the ease of comprehension, the proposed framework can be implemented in different traffic scenarios like roundabouts [17], highway on-ramps [13], etc. We denote the area illustrated by the red square of dimension S in Fig. 1 as the *merging zone* where possible collision may occur. Upstream of the merging zone, we define a *control zone* of length L , where CAVs can coordinate with each other before they pass the merging zone. The intersection has a coordinator that can communicate with the CAVs traveling inside the control zone. Note that the coordinator is not involved in any decision making process. When a vehicle enters the control zone, the coordinator receives its information and assigns a unique identity $i \in \mathbb{N}$ to it. We denote the queue of the vehicles to be entering the merging zone as $\mathcal{N}(t)$. The objective of each CAV is to derive its optimal control input (acceleration/deceleration) to cross the merging zone avoiding collision with the other vehicles, and without violating any of the state and control constraints.

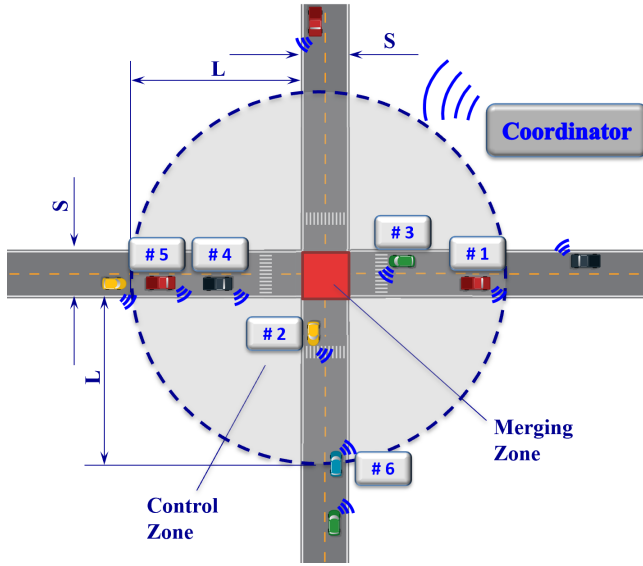


Fig. 1. A traffic network of CAVs approaching a four-way intersection.

A. Vehicle Dynamics and Constraints

We model each vehicle $i \in \mathcal{N}(t)$ as a double integrator

$$\begin{aligned} \dot{p}_i &= v_i(t) \\ \dot{v}_i &= u_i(t) \end{aligned} \quad (1)$$

where $p_i(t) \in \mathcal{P}_i$, $v_i(t) \in \mathcal{V}_i$, and $u_i(t) \in \mathcal{U}_i$ denote the position, speed and acceleration (control input) of each vehicle i in the corridor. The sets \mathcal{P}_i , \mathcal{V}_i , and \mathcal{U}_i , $i \in \mathcal{N}(t)$,

are complete and totally bounded subsets of \mathbb{R} . Let $\mathbf{x}_i(t) = [p_i(t) \ v_i(t)]^T$ denote the state vector of each vehicle i , with initial value $\mathbf{x}_i^0 = [p_i^0 \ v_i^0]^T$ taking values in $\mathcal{X}_i = \mathcal{P}_i \times \mathcal{V}_i$. The state space \mathcal{X}_i for each vehicle i is closed with respect to the induced topology on $\mathcal{P}_i \times \mathcal{V}_i$ and thus, it is compact. Each CAV i enters the control zone at t_i^0 , enters the merging zone at t_i^m , and exists the merging zone at t_i^f .

To ensure that the control input and vehicle speed are within a given admissible range, the following constraints are imposed.

$$\begin{aligned} u_{min} &\leq u_i(t) \leq u_{max}, \quad \text{and} \\ 0 &\leq v_{min} \leq v_i(t) \leq v_{max}, \quad \forall t \in [t_i^0, t_i^f], \end{aligned} \quad (2)$$

where u_{min} , u_{max} are the minimum and maximum acceleration for each vehicle $i \in \mathcal{N}(t)$, and v_{min} , v_{max} are the minimum and maximum speed limits respectively.

To ensure the absence of rear-end collision of two consecutive vehicles traveling on the same lane, we impose the rear-end safety constraint

$$s_i(t) = p_k(t) - p_i(t) \geq \delta_i(t), \quad \forall t \in [t_i^0, t_i^f], \quad (3)$$

where $s_i(t)$ denotes the distance of vehicle i from vehicle k which is physically immediately ahead of i , and $\delta_i(t)$ minimum safe distance which is a function of speed $v_i(t)$.

For each CAV $i \in \mathcal{N}(t)$, the lateral collision is possible within the set Γ_i ,

$$\Gamma_i \triangleq \{t \mid t \in [t_i^m, t_i^f]\}. \quad (4)$$

Lateral collision between any two CAVs $i, j \in \mathcal{N}(t)$ can be avoided if the following constraint hold,

$$\Gamma_i \cap \Gamma_j = \emptyset, \quad \forall t \in [t_i^m, t_i^f], \quad i, j \in \mathcal{N}(t). \quad (5)$$

In the modeling framework described above, we impose the following assumption:

Assumption 1: Each vehicle is equipped with sensors to measure and share their local information while communication among CAVs occurs without any delays or errors.

Assumption 1 may be strong, but it is relatively straightforward to relax as long as the noise in the measurements and/or delays is bounded. For example, we can determine upper bounds on the state uncertainties as a result of sensing or communication errors and delays, and incorporate these into more conservative safety constraints.

B. Upper Level Vehicle Coordination

Let $N(t) \in \mathbb{N}$ be the number of CAVs inside the control zone at time $t \in \mathbb{R}^+$. When a vehicle enters the control zone, the coordinator receives its information and assigns a unique identity i to the vehicle. We denote the sequence of the vehicles to be entering the merging zone as $\mathcal{N}(t) = 1, \dots, N(t)$ and refer to this as the merging sequence. The sequence $\mathcal{N}(t)$ can be the outcome of an upper-level optimization problem. In what follows, we assume that the solution of the upper-level problem for determining the time t_i^m that each CAV enters the merging zone is given, and we will focus on a lower level control problem that will yield for each CAV the optimal control input to achieve the assigned t_i^m .

C. Lower Level Energy Optimization Problem

For each vehicle $i \in \mathcal{N}(t)$ traveling inside the control zone, we formulate an optimal control problem for each CAV i as,

$$\min_{u_i \in \mathcal{U}_i} J_i(u(t)) = \int_{t_i^0}^{t_i^m} C_i(u_i(t)) dt, \quad (6)$$

subject to : (1), (2), $p_i(t_i^0) = 0$, $p_i(t_i^m)$,
and given t_i^0 , $v_i(t_i^0)$, t_i^m .

Here, $C_i(u_i(t))$ is a function of the control input $u_i(t)$ and can be viewed as a measure of energy. When $C_i(u_i(t))$ is considered as the L^2 -norm of the control input, i.e. $C_i(u_i(t)) = \frac{1}{2}u_i^2(t)$, the transient engine operation can be minimized which, eventually, represents the minimization of energy consumption [3]. Note that, we do not provide any endpoint constraint of the speed $v_i(t_i^m)$. Additionally, we do not explicitly include the lateral (5) and rear-end (3) safety constraints. We enforce the lateral collision constraint by selecting the appropriate merging time t_i^m for each CAV i by solving the upper-level vehicle coordination problem. The activation of rear-end safety constraint can be avoided under proper initial conditions $[t_i^0, v_i^0(t)]$ as in [18].

From (6) and the state equations (1), we formulate the Hamiltonian function, $H_i(t, \boldsymbol{\lambda}(t), \mathbf{x}(t), u(t))$, for each vehicle $i \in \mathcal{N}(t)$,

$$H_i(t, \boldsymbol{\lambda}(t), \mathbf{x}(t), u(t)) = \frac{1}{2}u_i^2 + \lambda_i^p \cdot v_i + \lambda_i^v \cdot u_i, \quad (7)$$

where $\boldsymbol{\lambda}(t) = [\lambda_i^p \ \lambda_i^v]^T$ is the co-state vector consisting of the co-state components λ_i^p and λ_i^v corresponding to the state vector $\mathbf{x}_i(t)$. With the final terminal conditions at hand, we construct the endpoint Lagrangian $\bar{E}(t, \mathbf{x}(t), \boldsymbol{\nu})$,

$$\bar{E}(t, \mathbf{x}(t), \boldsymbol{\nu}) = \nu_i^1 (p_i^m - p_i(t_i^m)), \quad (8)$$

where ν_i^1 is a scalar for the endpoint constraint given in (6). If we include the state and control constraints in (2), the Lagrangian, $L_i(t, \boldsymbol{\lambda}(t), \boldsymbol{\mu}(t), \mathbf{x}(t), u(t))$, of the Hamiltonian is

$$\begin{aligned} L_i(t, \boldsymbol{\lambda}(t), \boldsymbol{\mu}(t), \mathbf{x}(t), u(t)) &= \frac{1}{2}u_i^2 \quad (9) \\ &+ \lambda_i^p \cdot v_i + \lambda_i^v \cdot u_i + \boldsymbol{\mu}^T \mathbf{g}(t, \mathbf{x}(t), u(t)) \\ &= \frac{1}{2}u_i^2 + \lambda_i^p \cdot v_i + \lambda_i^v \cdot u_i \\ &+ \mu_i^a \cdot (u_i - u_{max}) + \mu_i^b \cdot (u_{min} - u_i) \\ &+ \mu_i^c \cdot (v_i - v_{max}) + \mu_i^d \cdot (v_{min} - v_i), \quad \forall i \in \mathcal{N}(t) \end{aligned}$$

where, $\mathbf{g}(t, \mathbf{x}(t), u(t))$ corresponds to the path constraints,

$$\mathbf{g}(t, \mathbf{x}(t), u(t)) = \begin{cases} u_i(t) - u_{max} \leq 0, \\ u_{min}(t) - u_i(t) \leq 0, \\ v_i(t) - v_{max} \leq 0, \\ v_{min}(t) - v_i(t) \leq 0, \end{cases} \quad (10)$$

and $\boldsymbol{\mu}^T$ is the path co-vector consisting of the Lagrange multipliers,

$$\mu_i^a = \begin{cases} > 0, & u_i(t) - u_{max} = 0, \\ = 0, & u_i(t) - u_{max} < 0, \end{cases} \quad (11)$$

$$\mu_i^b = \begin{cases} > 0, & u_{min} - u_i(t) = 0, \\ = 0, & u_{min} - u_i(t) < 0, \end{cases} \quad (12)$$

$$\mu_i^c = \begin{cases} > 0, & v_i(t) - v_{max} = 0, \\ = 0, & v_i(t) - v_{max} < 0, \end{cases} \quad (13)$$

$$\mu_i^d = \begin{cases} > 0, & v_{min} - v_i(t) = 0, \\ = 0, & v_{min} - v_i(t) < 0. \end{cases} \quad (14)$$

The Euler-Lagrange equations are

$$\dot{\lambda}_i^p(t) = -\frac{\partial L_i}{\partial p_i} = 0, \quad (15)$$

$$\dot{\lambda}_i^v = -\frac{\partial L_i}{\partial v_i} = \begin{cases} -\lambda_i^p, & v_i(t) - v_{max} < 0 \text{ and} \\ & v_{min} - v_i(t) < 0, \\ -\lambda_i^p - \mu_i^c, & v_i(t) - v_{max} = 0, \\ -\lambda_i^p + \mu_i^d, & v_{min} - v_i(t) = 0, \end{cases} \quad (16)$$

and

$$\frac{\partial L_i}{\partial u_i} = u_i + \lambda_i^v + \mu_i^a - \mu_i^b = 0. \quad (17)$$

D. Unconstrained Optimization

Applying the necessary condition, the optimal control can be given

$$u_i(t) + \lambda_i^v = 0, \quad i \in \mathcal{N}(t). \quad (18)$$

From (15) and (16) we have $\lambda_i^p(t) = a_i$, and $\lambda_i^v(t) = -(a_i \cdot t + b_i)$. The coefficients a_i and b_i are constants of integration corresponding to each vehicle i . From (18) the optimal control input (acceleration/deceleration) as a function of time is given by

$$u_i^*(t) = a_i \cdot t + b_i, \quad \forall t \geq t_i^0. \quad (19)$$

Substituting the last equation into (1) we find the optimal speed and position for each vehicle, namely

$$v_i^*(t) = \frac{1}{2}a_i \cdot t^2 + b_i \cdot t + c_i, \quad \forall t \geq t_i^0 \quad (20)$$

$$p_i^*(t) = \frac{1}{6}a_i \cdot t^3 + \frac{1}{2}b_i \cdot t^2 + c_i \cdot t + d_i, \quad \forall t \geq t_i^0. \quad (21)$$

Here, a_i , b_i , c_i , and d_i are constants of integration. These four constants above can be computed by using the boundary conditions in (6).

III. CONSTRAINED OPTIMIZATION

To derive a closed-form analytical solution for (9), we (1) identify the conditions for constraint(s) exclusion, (2) define the condition under which they become active, and (3) derive the constrained optimal solution, if one exists.

A. Condition of Constraint Exclusion

Although we have two state and two control constraints from (10), there are 15 constraint combinations in total that can be activated. In this section, we show that it is only possible for a subset of the constraints to be active within an unconstrained solution. Therefore, it is not necessary to consider all the cases in the constrained problem. In what follows, we delve deeper into the nature of the unconstrained optimal arc to derive useful information about the possible existence of constraint activation within the control zone.

Lemma 1: If $v_i(t_i^m)$ is not fixed, then

$$t_i^m = -\frac{b_i}{a_i}. \quad (22)$$

Proof: We construct the endpoint Lagrangian $\bar{E}(t, \mathbf{x}(t), \boldsymbol{\nu})$ as in (8). We have the following terminal transversality conditions [19],

$$\lambda_i^p(t_i^m) = \frac{\partial \bar{E}}{\partial p_i} = \nu_i, \quad (23)$$

$$\lambda_i^v(t_i^m) = \frac{\partial \bar{E}}{\partial v_i} = 0. \quad (24)$$

Using the result of (24) in (19), we note,

$$u_i(t_i^m) = a_i t_i^m + b_i = 0, \quad (25)$$

which yields, (22). \blacksquare

Corollary 1: The constants b_i and a_i always have opposite signs.

Lemma 2: The optimal acceleration profile is linearly decreasing if,

$$v_i^0 < \frac{(p_i(t_i^m) - p_i(t_i^0))}{t_i^m}. \quad (26)$$

Similarly, the optimal acceleration profile is linearly increasing if,

$$v_i^0 > \frac{(p_i(t_i^m) - p_i(t_i^0))}{t_i^m}. \quad (27)$$

Proof: From (20) and (21), we can write

$$v_i(t_i^0) = v_i^0 = \frac{1}{2}a_i(t_i^0)^2 + b_i t_i^0 + c_i. \quad (28)$$

$$p_i(t_i^0) = \frac{1}{6}a_i \cdot (t_i^0)^3 + \frac{1}{2}b_i \cdot (t_i^0)^2 + c_i \cdot t_i^0 + d_i. \quad (29)$$

Let $t_i^0 = 0$, then we get

$$c_i = v_i^0, \quad (30)$$

$$d_i = p_i(t_i^0). \quad (31)$$

From (21), we have,

$$p_i(t_i^m) = \frac{1}{6}a_i(t_i^m)^3 + \frac{1}{2}b_i(t_i^m)^2 + c_i t_i^m + d_i. \quad (32)$$

Using the results from (30), (31) and (22) in (32) and solving for a_i , we get

$$a_i = \frac{3(v_0 t_i^m - (p_i(t_i^m) - p_i(t_i^0)))}{(t_i^m)^3}. \quad (33)$$

Since $t_i^m > 0$, a_i is non positive if

$$v_i^0 t_i^m - (p_i(t_i^m) - p_i(t_i^0)) < 0, \quad (34)$$

which in turn implies negative slope of the acceleration profile, i.e., linearly decreasing acceleration profile. The second part of Lemma 2 can be proved following similar steps. \blacksquare

Lemma 3: For a given unconstrained optimal profile, only a subset of state-control constraints can remain active. Furthermore, if any element of the constraint pairs $v_i(t) - v_{max} \leq 0$, $u_i(t) - u_{max} \leq 0$ is activated, none of the constraint pairs $v_{min} - v_i(t) \leq 0$, $u_i(t) - u_{min} \geq 0$ can be activated. The reverse also holds.

Proof: The optimal solution derived from the unconstrained Hamiltonian analysis yields a linear control profile increasing or decreasing to the terminal value zero (Lemma 2). In the case where the acceleration profile is linearly decreasing, we have $u_i(t) = a_i t + b_i \geq 0 > u_{min}$, for all $t \in [t_i^0, t_i^m]$, implying that the constraint $u_i(t) - u_{min}(t) \geq 0$ will never be activated. Thus, $\mu_i^b = 0$, for all $t > t_i^0$ in (12). The corresponding quadratic velocity profile (20) is a parabolic function of degree 2 with y-symmetric axis located at t_i^m in the speed-time profile. Applying the necessary and sufficient condition of optimality in (20), we get,

$$\frac{\partial v_i(t)}{\partial t} = a_i t + b_i = 0, \quad (35)$$

$$\frac{\partial^2 v_i(t)}{\partial t^2} = a_i. \quad (36)$$

Solving (35), we have the inflection point at $t = -\frac{b_i}{a_i}$ which corresponds to the vertex of the parabola of (20). Whether this point corresponds to the maximum or minimum of the (20) can be determined from the sufficient condition of (36). For $a_i < 0$, we have a maximum at the vertex, giving rise to a concave quadratic profile. As the inflection point is located at t_i^m and $v_{min} < v_i^0 < v_{max}$, we have $v_i(t) > v_{min}$, for all $t \geq t_i^0$. Therefore, for a CAV with linearly decreasing unconstrained optimal acceleration profile, the constraint $v_i(t) - v_{min}(t) \geq 0$ and $u_i(t) - u_{min} \geq 0$ will not be activated.

The second part of Lemma 3 can be proved following similar arguments. Due to space limitation the proof is omitted. \blacksquare

Remark : The sign of the constant a_i provides insight for the possible state and control constraint activation.

Based on Lemmas 2 and 3, the following result provides the condition under which the state and control constraints never become active.

Theorem 1: The state constraint $v_i(t) - v_{min} \geq 0$ and the control constraint $u_i(t) - u_{min} \geq 0$ is not activated when $v_i^0 < \frac{(p_i(t_i^m) - p_i(t_i^0))}{t_i^m}$ holds. Similarly, the state constraint $v_{max} - v_i(t) \geq 0$ and the control constraint $u_{max} - u_i(t) \geq 0$ is not activated, if $v_i^0 > \frac{(p_i(t_i^m) - p_i(t_i^0))}{t_i^m}$ holds.

Proof: If $v_i^0 < \frac{(p_i(t_i^m) - p_i(t_i^0))}{t_i^m}$ holds, then according to Lemma 2, a_i is negative and the optimal acceleration profile is linearly decreasing. From Lemma 3, a decreasing acceleration profile indicates that the state constraint $v_i(t) - v_{min}(t) \geq 0$ and the control constraint $u_i(t) - u_{min}(t) \geq 0$

will never be activated, which concludes the proof of the first part.

The second part of Theorem 1 can be proved following similar arguments. Due to space limitation the proof is omitted. ■

B. Conditions of Constraint activation

The following results provide the condition for which the activation of the state and control constraints exists.

Lemma 4: activation of the control constraint $u_i(t) - u_{max} \leq 0$ or $u_i(t) - u_{min} \geq 0$ occurs at time $t = t_i^0$.

Proof: For $a_i < 0$, there is possibility of either the state constraint $v_i(t) - v_{max}(t) \leq 0$ or the control constraint $u_i(t) - u_{max} \leq 0$ or both to be activated (Lemma 3). In this case, Lemma 2 implies that the slope of the acceleration profile will be negative, i.e., linearly decreasing to zero. Therefore, any activation of the control constraint $u_i(t) - u_{max}(t) \leq 0$, if exists, will occur at time $t = t_i^0$. Similarly, it can be proved that the activation of $u_i(t) - u_{min} \geq 0$ occurs at time $t = t_i^0$. ■

Theorem 2: For $a_i < 0$, the state constraint $v_i(t) - v_{max}(t) \leq 0$ is activated if

$$t_i^m < \frac{3(p_i(t_i^m) - p_i(t_i^0))}{v_i^0 + 2v_{max}}. \quad (37)$$

Similarly, for $a_i > 0$, the activation of the state constraint $v_i(t) - v_{min}(t) \geq 0$ exists if

$$t_i^m > \frac{3(p_i(t_i^m) - p_i(t_i^0))}{v_i^0 + 2v_{min}}. \quad (38)$$

Proof: Let us consider that for $a_i < 0$, there exists a time $\tau_s \in [t_i^0, t_i^m]$ at which the state constraint $v_i(t) - v_{max}(t) \leq 0$ is activated. Using (30) as in Lemma 1, we write (20) as,

$$\frac{1}{2}a_i\tau_s^2 + b_i\tau_s + v_i^0 = v_{max}. \quad (39)$$

Solving for τ_s , we get

$$\tau_s = \frac{-2b_i \pm \sqrt{4b_i^2 - 8a_i(v_i^0 - v_{max})}}{2a_i} \quad (40)$$

Using (22), we have two possible solutions of τ ,

$$\tau_s = t_i^m + \sqrt{\frac{4b_i^2 - 8a_i(v_i^0 - v_{max})}{4a_i^2}}, \quad (41)$$

$$\tau_s = t_i^m - \sqrt{\frac{4b_i^2 - 8a_i(v_i^0 - v_{max})}{4a_i^2}}. \quad (42)$$

Now, (41) is not feasible since $\sqrt{4b_i^2 - 8a_i(v_i^0 - v_{max})}$ cannot be negative or equal to zero to satisfy $\tau_s < t_i^m$. Therefore, (42) is the acceptable solution. To satisfy $\tau_s < t_i^m$, $\sqrt{4b_i^2 - 8a_i(v_i^0 - v_{max})} > 0$. Simplifying, we have

$$a_i < \frac{2(v_i^0 - v_{max})}{t_i^m}. \quad (43)$$

Substituting (33), we have (37). By considering $a_i > 0$, the same procedure can be used to prove (38) of Theorem 2. ■

Theorem 3: If $a_i < 0$, the control constraint $u_i(t) - u_{max}(t) \leq 0$ is activated if,

$$t_i^m < \frac{-3v_i^0 + \sqrt{9(v_i^0)^2 + 12u_{max}(p_i(t_i^m) - p_i(t_i^0))}}{2u_{max}}. \quad (44)$$

For $a_i > 0$, control constraint $u_{min} - u_i(t) \leq 0$ is activated if,

$$t_i^m > \frac{-3v_i^0 + \sqrt{9(v_i^0)^2 + 12u_{min}(p_i(t_i^m) - p_i(t_i^0))}}{2u_{min}}. \quad (45)$$

Proof: Based on Lemma 4, the control constraint activation occurs at $t = t_i^0$. For $a_i < 0$, we have,

$$u_i(t_i^0) = a_i t_i^0 + b_i > u_{max}. \quad (46)$$

With $t_i^0 = 0$, we get $b_i = -a_i t_i^m > u_{max}$. Substituting a_i from (33), we obtain

$$u_{max}(t_i^m)^2 + 3v_i^0 t_i^m - 3(p_i(t_i^m) - p_i(t_i^0)) < 0. \quad (47)$$

Solving the quadratic term for t_i^m , we eventually obtain

$$\left(t_i^m + \frac{3v_i^0 + \sqrt{9(v_i^0)^2 + 12u_{max}(p_i(t_i^m) - p_i(t_i^0))}}{2u_{max}}\right) \left(t_i^m + \frac{3v_i^0 - \sqrt{9(v_i^0)^2 + 12u_{max}(p_i(t_i^m) - p_i(t_i^0))}}{2u_{max}}\right) < 0. \quad (48)$$

The first term of (48) is always positive as $\sqrt{9(v_i^0)^2 + 12u_{max}(p_i(t_i^m) - p_i(t_i^0))} > 0$. Therefore, the second part has to be negative which yields the condition stated in (44). For $a_i > 0$, (45) can be proved with similar procedure. ■

We have discussed so far the conditions under which the state and control constraints are activated individually. With this information, we can solve the constrained optimization problem and derive corresponding analytical solution, which we will present in the following section. However, there is a possibility that the optimal solution might result in additional constraint activation that was nonexistent in the initial estimation. For example, the solution of the optimization problem with only state constraint might cause additional control constraint activation. Similarly, resolving the control constrained problem might result in state constraint activation. In such cases, the optimization problem has to be resolved with updated constraints to derive the corresponding analytical solution. As our goal is to derive and implement the solution online, this procedure is not computationally feasible. Therefore, we need to check beforehand under which condition these additional constraints may be activated.

Theorem 4: If the state constraint $v_i(t) - v_{max} \leq 0$ is activated, then the state constrained optimal solution results in additional control constraint $u_i(t) - u_{max} \leq 0$ activation if,

$$\tau_s < \frac{-3v_i^0 + \sqrt{9(v_i^0)^2 + 12u_{max}(p_i(\tau_s) - p_i(t_i^0))}}{2u_{max}}. \quad (49)$$

Here, τ_s is the time at which the state constraint transits from unconstrained to the constrained arc and can be calculated from the terminal conditions. Similarly, if the state constraint $v_i(t) - v_{min} \geq 0$ is activated, then the state constrained

optimal solution results in an additional control constraint $u_i(t) - u_{min} \geq 0$ activation if,

$$\tau_s > \frac{-3v_i^0 + \sqrt{9(v_i^0)^2 + 12u_{min}(p_i(\tau_s) - p_i(t_i^0))}}{2u_{min}}. \quad (50)$$

Proof: Let's assume that the state constraint $v_i(t) - v_{max} \geq 0$ is activated at $t = \tau_s$. The state constrained optimal solution yields a linear acceleration profile that has to enter the constrained arc at $t = \tau_s$ with $u_i(\tau_s) = 0$. As a result, we can focus on the unconstrained state and control trajectory with reduced time horizon $t \in [t_i^0, \tau_s]$ instead of $[t_i^0, t_i^m]$. Following the same procedure from the proof of theorem 4, we can construct the condition (49) that indicates whether the control constraint $u_i(t) - u_{max} \leq 0$ is being activated within the modified horizon $t \in [t_i^0, \tau_s]$.

The second part of Theorem 4 can be proved following similar arguments. Due to space limitation the proof is omitted. ■

Theorem 5: If the control constraint $u_i(t) - u_{max} \leq 0$ is activated, then the control constrained optimal solution results in additional state constraint $v_i(t) - v_{max} \leq 0$ activation, if the following condition holds

$$t_i^m < \tau_c + \frac{3(p_i(t_i^m) - p_i(\tau_c))}{v_i^0 + u_{max}\tau_c + 2v_{max}}. \quad (51)$$

Here, τ_c is the time at which the control constraint transits from the constrained to the unconstrained arc. Similarly, If the control constraint $u_i(t) - u_{min} \geq 0$ is activated first, then the control constrained optimal solution results in additional state constraint $v_i(t) - v_{min} \geq 0$ activation if the following holds,

$$t_i^m > \tau_c + \frac{3(p_i(t_i^m) - p_i(\tau_c))}{v_i^0 + u_{min}\tau_c + 2v_{min}}. \quad (52)$$

Proof: Let's assume that the control constraint $u_i(t) - u_{max} \leq 0$ is activated first. The control constrained optimal solution yields an acceleration profile that exits the constrained arc at $t = \tau_c > t_i^0$ with $u_i(\tau_c) = u_{max}$. Therefore, we can focus on the unconstrained state and control trajectory with reduced time horizon $t \in [\tau_c, t_i^m]$ instead of $[t_i^0, t_i^m]$. Following the same procedure as in the proof of Theorem 2, we can construct the condition (49).

Following similar arguments, we can proof (52). Due to space limitation the proof is omitted. ■

IV. ANALYTICAL SOLUTION OF CONSTRAINED OPTIMIZATION

To derive the analytical solution of (6) using Hamiltonian analysis, we follow the standard methodology used in optimal control problems with control and state constraints [19] and [20]. We first start with Theorem 1 to reduce the set of possible constraint activations. Then we evaluate the conditions in Theorem 2 and 3 to check for possible constraint activation. If no activation is identified, we simply derive the unconstrained arc. If any constraint activation is detected by checking the conditions in Theorem 2 and 3, we then further check the conditions in Theorem 4 and 5 to identify any additional constraint activation that might ensue from the previous case. Once the nature of the current

and additional constraint activation is specified, we then piece together the relevant unconstrained and constrained arcs that yield a set of algebraic equations which are solved simultaneously using the boundary conditions of and interior conditions between the arcs.

We now consider the different cases of state and control constraint activations to derive the optimal profile for the CAVs. Due to space limitation, we only present derivation pertaining to the state constraint $v_i(t) - v_{max}(t) \leq 0$ and control constraint $u_i(t) - u_{max}(t) \leq 0$ activation.

Case 1: If only the state constraint $v_i(t) - v_{max} \leq 0$ is activated, we have $\mu_i^a = \mu_i^b = \mu_i^d = 0$. The corresponding necessary condition for optimality, and the Euler-Lagrangian equations (15) and (16) for the costates become

$$u_i + \lambda_i^v = 0, \quad (53)$$

$$\dot{\lambda}_i^p = 0, \quad (54)$$

$$\dot{\lambda}_i^v = -\lambda_i^p - \mu_i^c. \quad (55)$$

Let us assume that at a time τ_s such that $t_i^0 < \tau_s < t_i^m$, the state constraint is activated. We have an interior boundary condition $\mathbf{g}(\tau_s, \mathbf{x}(\tau_s)) = v_i(\tau_s) - v_{max} = 0$, and have a three-point boundary value problem. Therefore, at $t = \tau_s$, the state enters the constrained arc with $v_i(t) = v_{max}$. We denote τ_s^- and τ_s^+ as the immediate left and the right side of τ_s . At this entry point, we need to consider the jump conditions to assess the discontinuities of the costates and Hamiltonian as,

$$\lambda(\tau_s^-) - \lambda(\tau_s^+) = \eta \frac{\partial \mathbf{g}(t, \mathbf{x}(t))}{\partial \mathbf{x}} \Big|_{t=\tau_s}, \quad (56)$$

$$H(\tau_s^+) - H(\tau_s^-) = \eta \frac{\partial \mathbf{g}(t, \mathbf{x}(t))}{\partial t} \Big|_{t=\tau_s}, \quad (57)$$

$$(58)$$

where, η is a constant Lagrange multipliers. Using (56) and (57), we determine the jump conditions of the costates and the Hamiltonian,

$$\lambda_i^p(\tau_s^-) - \lambda_i^p(\tau_s^+) = \eta \frac{\partial(v_i(\tau_s) - v_{max})}{\partial p_i(t)}, \quad (59)$$

$$\lambda_i^v(\tau_s^-) - \lambda_i^v(\tau_s^+) = \eta \frac{\partial(v_i(\tau_s) - v_{max})}{\partial v_i(t)}, \quad (60)$$

$$H(\tau_s^+) - H(\tau_s^-) + \eta \frac{\partial(v_i(\tau_s) - v_{max})}{\partial t}. \quad (61)$$

Note that, (59)-(61) imply possible discontinuity of the costates and the Hamiltonian at $t = \tau_s$, whereas the state variables remain continuous, i.e., $\mathbf{x}(\tau_s^-) = \mathbf{x}(\tau_s^+)$. From (59) and (61), both the position costate and the Hamiltonian is continuous at $t = \tau_s$. If $u_i(\tau_s^-) = 0$, then (61) yields $u_i(\tau_s^+) = 0$, which implies that $\lambda_i^v(t)$ is also continuous at $t = \tau_s$ and $\eta = 0$ in (60). Therefore, from (55), we have

$$\mu_i^c(t) = \begin{cases} 0, & \text{if } v_i(t) < v_{max}, \\ -\lambda_i^p, & \text{if } v_i(t) = v_{max}. \end{cases} \quad (62)$$

Using (53), (54), (55), (62), the initial, final conditions, and the terminal transversality condition at $t = t_i^m$, we

now formulate a closed form analytical solution stitching the unconstrained and constrained arcs together at $t = \tau_s$

$$\begin{pmatrix} \frac{(t_i^0)^2}{2} & \frac{(t_i^0)}{2} & 1 & 0 & 0 & 0 & 0 & 0 & 0 \\ \frac{(t_i^0)^3}{6} & \frac{(t_i^0)^2}{2} & t_i^0 & 1 & 0 & 0 & 0 & 0 & 0 \\ \tau_s & 1 & 0 & 0 & -\tau_s & -1 & 0 & 0 & 0 \\ \frac{\tau_s^2}{2} & \tau_s & 1 & 0 & 0 & 0 & 0 & 0 & 0 \\ \tau & 1 & 0 & 0 & 0 & 0 & 0 & 0 & 0 \\ \frac{\tau^2}{2} & \tau_s & 0 & 0 & -\frac{\tau^2}{2} & -\tau_s & 0 & 0 & 0 \\ 0 & 0 & 0 & 0 & \frac{(t_i^m)^3}{6} & \frac{(t_i^m)^2}{2} & t_i^m & 1 & 0 \\ 0 & 0 & 0 & 0 & t_i^m & 1 & 0 & 0 & 0 \end{pmatrix} \cdot \begin{pmatrix} a_i \\ b_i \\ c_i \\ d_i \\ e_i \\ f_i \\ g_i \\ h_i \end{pmatrix} = \begin{pmatrix} p_i(t_i^0) \\ v_i(t_i^0) \\ 0 \\ v_{max} \\ 0 \\ 0 \\ p_i(t_i^m) \\ 0 \end{pmatrix}, \forall t \geq t_i^0, \quad (63)$$

where a_i, b_i, c_i, d_i are the constants of integration for the unconstrained arc, and g_i, h_i, q_i, w_i are the constants of integration for the constrained arc.

Case 2: If only the control constraint $u_i(t) - u_{max} \leq 0$ is activated, we have $\mu_i^b = \mu_i^c = \mu_i^d = 0$. The corresponding necessary condition for optimality, and the Euler-Lagrangian equations (15) and (16) for the costates become

$$u_i + \lambda_i^v + \mu_i^a = 0, \quad (64)$$

$$\dot{\lambda}_i^p = 0, \quad (65)$$

$$\dot{\lambda}_i^v = -\lambda_i^p. \quad (66)$$

Let us assume that at a time $\tau_c > t_i^0$, the vehicle leaves the constrained arc. We denote τ_c^- and τ_c^+ as the immediate left and the right side of τ_c . At this entry point, using the jump conditions (56) and (57), we assess the discontinuities of the costates and the Hamiltonian,

$$\lambda_i^p(\tau_c^-) - \lambda_i^p(\tau_c^+) = \eta \frac{\partial(u_i(\tau_c) - u_{max})}{\partial p_i(t)}, \quad (67)$$

$$\lambda_i^v(\tau_c^-) - \lambda_i^v(\tau_c^+) = \eta \frac{\partial(u_i(\tau_c) - u_{max})}{\partial v_i(t)}, \quad (68)$$

$$H(\tau_c^+) - H(\tau_c^-) = \eta \frac{\partial(u_i(\tau_c) - u_{max})}{\partial t}. \quad (69)$$

From (68), we get

$$u_i(\tau_c^+) = u_i(\tau_c^-) = u_{max}. \quad (70)$$

Using (64),(65), (66), (70), the initial, final conditions, and the terminal transversality condition at $t = t_i^m$, we can formulate a closed form analytical solution similar to (63) by stitching the constrained and unconstrained arcs together at $t = \tau_c$.

Case 3: If both the control constraint $u_i(t) - u_{max} \leq 0$ and state constraint $v_i(t) - v_{max} \leq 0$ are activated, we can derive the analytical solution following the procedure

described in the previous two cases. Due to lack of space, only the numerical result is shown in the following section (see Fig. 4).

V. SIMULATION RESULTS

We validate the analytical solution of the constrained optimization problem through numerical analysis in MATLAB. We select the initial and final position as $p_i(t_i^0) = 0$ m and $p_i(t_i^m) = 200$ m, and the initial velocity as $v_i(t_i^0) = 13.4$ m/s. We enforce maximum velocity $v_{max} = 21$ m/s and maximum acceleration $u_{max} = 1.4$ m/s². We present only the cases with the state constraint $v_i(t) - v_{max} \leq 0$ and control constraint $u_i(t) - u_{max} \leq 0$ activation.

Fig. 2 shows the unconstrained optimal trajectory for two different merging time t_i^m of 10 s and 20 s. As stated in Lemma 2, we observe two different types of optimal trajectories. This implies that based on the terminal conditions, a CAV may speed up, or slow down optimally to satisfy the boundary conditions. We also observed that both the predefined state and control constraints (for $a_i < 0$) are activated in Fig. 2 (top-left and right). We can save the com-

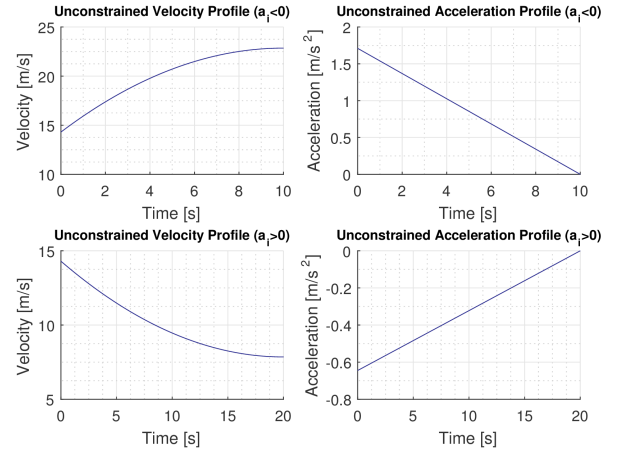


Fig. 2. State and control unconstrained optimal profile for 1) $a_i < 0$ (top) and 2) $a_i > 0$ (bottom) cases.

putational effort to produce the unconstrained results in Fig. 2 if any constraint is activated. Once we employ Theorem 1 to reduce possible constraint activation set, we use Theorem 2 and 3 to pinpoint the specific constraint activation case. We illustrate the optimal state and control trajectories for only state constrained in Fig. 3 (top) and only control constrained in Fig. 3 (bottom) cases. However, the results in Fig. 3 have to be recalculated if additional constraint activation is encountered. We can avoid the unnecessary computational effort to produce the intermediate result in Fig. 3 based on the following observation. Note that, in the state constrained solution, the control constraint is activated (Fig. 3, top-right) which was non-existent before, as discussed in theorem 4. Similarly, we observe in Fig. 3 (bottom-right) that the control constrained optimal trajectory creates a possibility of additional state constraint activation (Fig. 3, bottom-left) due to the increased speed, as discussed in Theorem 5. Hence, we

need to take the additional constraint activation into account by Theorem 4 and 5, and enforce both state and control constraints if needed. Fig. 4 shows the unconstrained and fully constrained state and control constrained trajectories. The three-point boundary value problem is solved in this case, and two constrained and one unconstrained arcs are pieced together to provide the optimal solution.

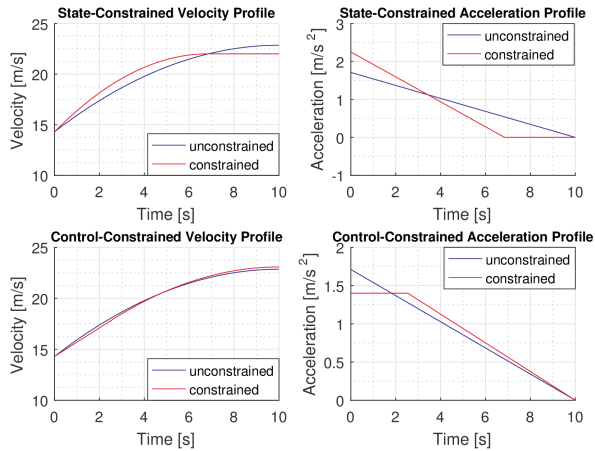


Fig. 3. State constrained optimal velocity (top-left) and acceleration (top-right) profile, and control constrained optimal velocity (bottom-left) and acceleration (bottom-right) profile.

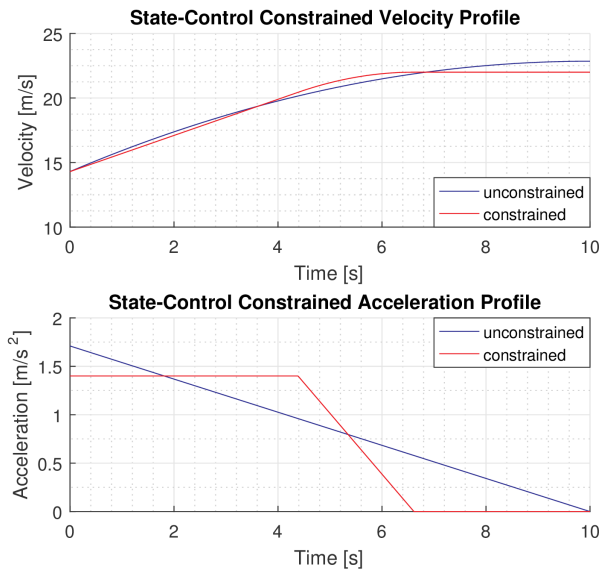


Fig. 4. State and control constrained optimal velocity (left) and acceleration (right) profile.

VI. CONCLUDING REMARKS

In this paper, we addressed the state and control constrained optimal framework for coordinated CAVs. We mathematically quantified the activation of the state-control constraints and provided conditions under which they become active. We derived the closed form analytical solution for

the constrained optimization problem and validated a subset of different cases through numerical simulation. Ongoing work includes other cases along with the conditions for the existence of solution along with the terminal speed constrained formulation.

REFERENCES

- [1] R. Margiotta and D. Snyder, "An agency guide on how to establish localized congestion mitigation programs," U.S. Department of Transportation. Federal Highway Administration, Tech. Rep., 2011.
- [2] J. Lee, B. B. Park, K. Malakorn, and J. J. So, "Sustainability assessments of cooperative vehicle intersection control at an urban corridor," *Transportation Research Part C: Emerging Technologies*, vol. 32, pp. 193–206, 2013.
- [3] A. A. Malikopoulos, C. G. Cassandras, and Y. J. Zhang, "A decentralized energy-optimal control framework for connected automated vehicles at signal-free intersections," *Automatica*, vol. 93, pp. 244 – 256, 2018.
- [4] A. A. Malikopoulos and J. P. Aguilar, "An Optimization Framework for Driver Feedback Systems," *IEEE Transactions on Intelligent Transportation Systems*, vol. 14, no. 2, pp. 955–964, 2013.
- [5] K. Dresner and P. Stone, "Multiagent traffic management: a reservation-based intersection control mechanism," in *Proceedings of the Third International Joint Conference on Autonomous Agents and Multiagents Systems*, 2004, pp. 530–537.
- [6] —, "A multiagent approach to autonomous intersection management," *Journal of artificial intelligence research*, vol. 31, pp. 591–656, 2008.
- [7] A. de La Fortelle, "Analysis of reservation algorithms for cooperative planning at intersections," *13th International IEEE Conference on Intelligent Transportation Systems*, pp. 445–449, Sep. 2010.
- [8] S. Huang, A. Sadek, and Y. Zhao, "Assessing the Mobility and Environmental Benefits of Reservation-Based Intelligent Intersections Using an Integrated Simulator," *IEEE Transactions on Intelligent Transportation Systems*, vol. 13, no. 3, pp. 1201–1214, 2012.
- [9] I. H. Zohdy, R. K. Kamalanathsharma, and H. Rakha, "Intersection management for autonomous vehicles using iCACC," *2012 15th International IEEE Conference on Intelligent Transportation Systems*, pp. 1109–1114, 2012.
- [10] F. Yan, M. Dridi, and A. El Moudni, "Autonomous vehicle sequencing algorithm at isolated intersections," *2009 12th International IEEE Conference on Intelligent Transportation Systems*, pp. 1–6, 2009.
- [11] K.-D. Kim and P. Kumar, "An MPC-Based Approach to Provable System-Wide Safety and Liveness of Autonomous Ground Traffic," *IEEE Transactions on Automatic Control*, vol. 59, no. 12, pp. 3341–3356, 2014.
- [12] J. Rios-Torres and A. A. Malikopoulos, "A Survey on Coordination of Connected and Automated Vehicles at Intersections and Merging at Highway On-Ramps," *IEEE Transactions on Intelligent Transportation Systems*, vol. 18, no. 5, pp. 1066–1077, 2017.
- [13] J. Rios-Torres, A. A. Malikopoulos, and P. Pisu, "Online Optimal Control of Connected Vehicles for Efficient Traffic Flow at Merging Roads," in *2015 IEEE 18th International Conference on Intelligent Transportation Systems*, 2015, pp. 2432–2437.
- [14] I. A. Ntousakis, I. K. Nikolos, and M. Papageorgiou, "Optimal vehicle trajectory planning in the context of cooperative merging on highways," *Transportation Research Part C: Emerging Technologies*, vol. 71, pp. 464–488, 2016.
- [15] Y. Zhang, A. A. Malikopoulos, and C. G. Cassandras, "Optimal control and coordination of connected and automated vehicles at urban traffic intersections," in *Proceedings of the American Control Conference*, 2016, pp. 6227–6232.
- [16] A. M. I. Mahbub, L. Zhao, D. Assanis, and A. A. Malikopoulos, "Energy-optimal coordination of connected and automated vehicles at multiple intersections," in *Proceedings of the American Control Conference*, 2019 (To Appear).
- [17] L. Zhao, A. A. Malikopoulos, and J. Rios-Torres, "Optimal control of connected and automated vehicles at roundabouts: An investigation in a mixed-traffic environment," in *15th IFAC Symposium on Control in Transportation Systems*, 2018, pp. 73–78.
- [18] A. A. Malikopoulos, S. Hong, B. Park, J. Lee, and S. Ryu, "Optimal control for speed harmonization of automated vehicles," *IEEE Transactions on Intelligent Transportation Systems*, vol. 20, no. 7, pp. 2405–2417, 2019.

- [19] I. M. Ross, *A Primer on Pontryagin's Principle in Optimal Control*. Collegiate Publishers, 2015.
- [20] A. E. Bryson and Y. C. Ho, *Applied optimal control: optimization, estimation and control*. CRC Press, 1975.